EDUCATUM JSMT Vol. 12 Number 1 (2026)
ISSN 2289-7070 / e-ISSN 2462-2451(1-23)
https://ejournal.upsi.edu.my/index.php/EJSMT/index

Computational Analysis of Fractional Systems of Korteweg-de Vries Equations Using Elzaki Projected Differential Transform Method

Sunday Oluwafemi Gbodogbe[1*], and Adedapo Chris Loyinmi[2]

[1]Department of Mathematical Sciences, Indiana University, Indianapolis, USA.

[2]Department of Mathematics, Tai Solarin University of Education, Ijebu-ode, Nigeria

**Corresponding author:* sgbogogb@iu.edu

Received: 18 February 2025; **Accepted:** 13 August 2025; **Published:** 4 January 2026

To cite this article (APA): Gbodogbe S.O and Loyinmi AC., (2026) Computational Analysis of Fractional Systems of Korteweg-de Vries Equations Using Elzaki Projected Differential Transform Method. EDUCATUM Journal of Science, Mathematics and Technology, 13(1), 1–23

To link to this article:

Abstract

This study investigates the application of the Elzaki Projected Differential Transform Method (EPDTM) to fractional-order nonlinear Korteweg-de Vries (KdV) equations, which describe various nonlinear wave phenomena in physics and engineering. The method effectively addresses both linear and nonlinear operators and fractional derivatives. Through two illustrative examples, the method accurately captures the dynamics of fractional-order wave systems and achieves results in excellent agreement with exact solutions. The findings demonstrate the method's precision, fast convergence, and computational efficiency, underscoring EPDTM's potential as a robust tool for solving nonlinear partial differential equations with fractional dynamics.

Keywords: Fractional Korteweg-de Vries equations, Elzaki transform, Projected Differential Transform Method, Fractional calculus, Numerical simulation

INTRODUCTION

The Korteweg-de Vries (KdV) equation is a fundamental mathematical model used to describe the behavior of weakly nonlinear long waves in various fields of physics and engineering. Its significance lies in its ability to capture the intricate balance between weak nonlinearity and weak dispersion, which governs wave evolution. The equation, named after Diederik Korteweg and Gustav de Vries, was introduced in their seminal 1895 paper, where they demonstrated its applicability to small-amplitude long waves on the free surface of water. Initially derived by Joseph Boussinesq in 1877, the KdV equation has since found applications far beyond its original context of shallow-water waves in canals. It plays a crucial role in explaining phenomena such as shock waves, traveling waves, and solitons in diverse areas including fluid dynamics, aerodynamics, and continuum mechanics [1-10]. The equation models processes like shock wave formation, turbulence, boundary layer behavior, and mass transport, making it an indispensable tool in theoretical and applied research. One of the most remarkable properties of the KdV equation is its exact solvability. This property was first highlighted by Gardner et al. in 1967, who showed that the KdV equation could be solved exactly as an initial-value problem with arbitrary initial data in a suitable function space. This discovery marked a revolution in the study of nonlinear partial differential equations, attracting significant scholarly attention. Notably, Zakharov and Faddeev demonstrated in 1971 that the KdV equation exemplifies an infinite-dimensional Hamiltonian system that is completely integrable [11-15]. The exact solutions of the KdV equation, often obtained using the inverse scattering transform, include solitons—stable, localized wave packets that maintain their shape while traveling at constant speeds. These solutions have made the KdV equation a prototypical example in the study of exactly solvable models in nonlinear dynamics. The mathematical richness and the intriguing physical properties of the KdV equation continue to inspire active research [15-20].

Fractional calculus (FC) extends the concept of traditional calculus by allowing derivatives and integrals to be of non-integer (fractional) order. This extension proves to be particularly effective in modeling complex engineering and physical systems where standard integer-order differential equations fall short. Unlike traditional models, fractional calculus (FC) offers a more precise representation of the dynamics involved in diverse phenomena spanning multiple disciplines. These include chemistry, economics, electrical engineering, control theory, groundwater issues, mechanics, signal and image processing, and biological sciences. In recent years, fractional differential equations have become instrumental in the study of nonlinear equations and their traveling-wave solutions. These solutions are essential for understanding nonlinear physical processes, which often involve intricate interactions and evolutions of waves [8, 10, 20-25]. The Korteweg-de Vries (KdV) equation, a cornerstone in the analysis of nonlinear wave phenomena, benefits significantly from the application of fractional calculus. By incorporating fractional derivatives, the KdV equation can model a broader spectrum of physical phenomena, providing a more comprehensive framework for studying the interaction and evolution of nonlinear waves. The application of fractional calculus to the KdV equation enhances its capability to describe various physical processes more accurately. This approach is particularly useful in situations where traditional models with integer-order derivatives are inadequate. As a result, fractional calculus has emerged as a powerful tool in advancing our understanding of complex systems governed by nonlinear dynamics. Through the integration of fractional calculus, researchers can develop more robust and versatile models of the KdV equation. These models not only improve our theoretical understanding but also have practical implications in fields ranging from fluid dynamics to quantum mechanics. The ongoing exploration of fractional-order KdV equations continues to reveal new insights and applications, underscoring the importance of this mathematical framework in modern scientific research [26-30].

The fractional-order coupled Korteweg-de Vries (KdV) equations extend the classical KdV framework by incorporating fractional derivatives, which allows for a more nuanced modeling of complex wave phenomena. These equations are defined as follows:

$$\frac{\partial^\alpha u}{\partial \theta^\alpha} = -c\frac{\partial^3 u}{\partial \psi^3} - 6cu\frac{\partial u}{\partial \psi} + 6v\frac{\partial v}{\partial \psi},$$

$$\frac{\partial^\alpha v}{\partial \theta^\alpha} = -c\frac{\partial^3 v}{\partial \psi^3} - 3du\frac{\partial v}{\partial \psi}, \qquad 0 < \alpha < 1$$

where c and d are constants, and α denotes the parameter that characterizes the order of the fractional derivatives of $u(\psi,\theta)$ and $v(\psi,\theta)$, respectively. The functions $u(\psi,\theta)$ and $v(\psi,\theta)$ represent the fundamental variables of space and time, and are considered to vanish for $\psi < 0$ and $\theta < 0$. When $c = d = 1$, this formulation simplifies to the traditional coupled Korteweg-de Vries (KdV) equations.

In the equations above $\frac{\partial^\alpha u}{\partial \theta^\alpha}$ and $\frac{\partial^\alpha v}{\partial \theta^\alpha}$ denote the fractional derivatives of order α. These derivatives are generalizations of the standard integer-order derivatives, providing a powerful tool to describe memory and hereditary properties inherent in various physical processes. Fractional derivatives are particularly effective in capturing the complex dynamics of systems where the influence of past states decays over time, which is a common characteristic in many natural and engineered systems. The constants

c and d play a crucial role in determining the characteristics of the wave propagation and interaction described by the equations. By adjusting these constants, one can model different physical scenarios and behaviors. The parameter α, which lies between 0 and 1, indicates the order of the fractional derivative. This parameter provides an additional degree of freedom in the model, allowing for a more flexible and accurate representation of the system's dynamics. The functions $u(\psi,\theta)$ and $v(\psi,\theta)$ are the primary variables representing the wave phenomena in space and time. These functions are assumed to be zero for negative values of ψ and θ, implying that the waves do not exist before the origin in space and time. This consideration is essential for ensuring the physical relevance of the solutions, as it aligns with the causality principle, where effects follow causes. When the constants c and d are set to 1, the fractional-order coupled KdV equations simplify to the classical coupled KdV equations. This reduction highlights the fractional-order equations' generality, encompassing the classical case as a specific instance. The classical coupled KdV equations are well-studied and known for describing the interaction of nonlinear waves, solitons, and other complex wave structures [1-5, 30-32].

Over the years, various researchers have proposed and developed numerous methods to solve the Korteweg-de Vries (KdV) equations, which model a wide range of nonlinear wave phenomena. Here, we review significant contributions to the solution of these equations: Maturi (2012) utilized the Adomian decomposition method to solve the Generalized Hirota–Satsuma coupled KdV equations [31]. By applying the differential transform technique, Gokdogan et al [36] studied approximate solutions for coupled KdV equations. This method transforms the differential equations into a series of algebraic equations, which can be solved iteratively to obtain approximate solutions. The analysis of nonlinear KdV equations using the Homotopy Analysis Method (HAM) was suggested by Jafari and Firoozjaee (2010) [39]. Lu et al. (2020) [40] employed fractional calculus by He's method to compute numerical solutions for a system of coupled nonlinear fractional Korteweg-de Vries (KdV) equations.

The Elzaki Projected Differential Transform Method (EPDTM) is proposed as a novel approach to solving fractional-order coupled KdV equations due to several compelling reasons. The EPDTM is designed to efficiently handle the nonlinearity and fractional nature of the equations. Traditional methods often struggle with the complexities introduced by fractional derivatives, but EPDTM can seamlessly incorporate these into the solution process. The EPDTM is known for its accuracy and rapid convergence, which are crucial for solving complex coupled equations. By projecting the differential transform method through the Elzaki transform, this method reduces computational errors and enhances solution precision. One of the primary advantages of the EPDTM is its ability to simplify the computational process. By transforming the problem into a series of algebraic equations, it reduces the difficulty associated with solving the original fractional differential equations directly. The EPDTM can be applied to a wide range of initial and boundary value problems, making it a versatile tool for various applications. Its adaptability to different types of fractional differential equations makes it particularly suitable for the fractional-order coupled KdV equations. The method provides enhanced analytical capabilities, allowing for a deeper understanding of the underlying physical phenomena. By obtaining more accurate and detailed solutions, researchers can better analyze the wave interactions and dynamics described by the fractional-order coupled KdV equations. The coupled nature of the fractional-order KdV equations necessitates a method that can effectively address the interaction between multiple variables. The EPDTM is well-suited for coupled systems, providing a robust framework for analyzing the interplay between the fundamental functions of space and time. By employing the Elzaki Projected Differential Transform Method, we aim to achieve a more comprehensive and precise analysis of the fractional-order coupled KdV equations, advancing our understanding of nonlinear wave phenomena and enhancing the applicability of these models in various scientific and engineering fields [2-7, 38-40].

Despite their wide use, many existing methods for solving fractional differential equations—such as the Adomian Decomposition Method (ADM), Homotopy Perturbation Method (HPM), and Variational Iteration Method (VIM)—encounter significant computational limitations. These approaches often rely on recursive correction steps, linearization, or perturbative assumptions, which can be time-consuming and difficult to implement for highly nonlinear or stiff systems. Moreover, the convergence of the resulting series may be slow or require many terms to approximate the solution accurately, thereby increasing computational overhead. In contrast, the Elzaki Projected Differential Transform Method (EPDTM) provides a direct, non-iterative framework that simplifies implementation, improves convergence speed, and offers higher numerical precision with reduced computational cost.

The EPDTM is utilized to investigate the fractional-order properties inherent in the system of Korteweg-de Vries (KdV) equations. Specific illustrative cases are examined to demonstrate the effectiveness of this approach. Results for both fractional-order and integral-order models are obtained using this technique. Moreover, this method proves beneficial for addressing a broad spectrum of fractional-order linear and nonlinear partial differential equations.

FRACTIONAL CALCULUS THEORY

In this study, we adopt the Caputo definition of fractional derivatives, as it allows for the use of classical initial conditions (in terms of integer-order derivatives), which makes it more suitable for physical and engineering applications compared to the Riemann–Liouville form.

Definition 1. The Riemann–Liouville fractional operator ${}^{RL}D^{\alpha}$ of order α is defined as follows [39, 40]:

$$ {}^{RL}D^{\alpha}u(\psi)=\begin{cases}\dfrac{d^i}{d\psi^i}u(\psi),\alpha=i\\ \dfrac{1}{\Gamma(i-\psi)}\dfrac{d^i}{d\psi^i}\displaystyle\int_0^{\alpha}\dfrac{u(\psi)}{(\psi-\rho)^{\alpha-i+1}}d\psi, i-1<\alpha<i\end{cases} \tag{1}$$

For $j\in Z^{+},\alpha\in R^{+}$, hence

$$ {}^{RL}D^{\alpha}u(\psi)=\frac{1}{\Gamma(\alpha)}\int_0^{\psi}(\psi-\rho)^{\alpha-1}f(\rho)d\rho, \tag{2}$$

where $0<\alpha\le 1$

Definition 2: The operator I^{α} of fractional-order Riemann–Liouville integration is formally defined as presented in references [39, 40].

$$ I^{\alpha}u(\psi)=\frac{1}{\Gamma(\alpha)}\int_0^{\psi}(\psi-\rho)^{\alpha-1}f(\rho)d\rho, \tag{3}$$

The fundamental properties of the operator are as follows:

$$ I^{\alpha}\psi^{i}=\frac{\Gamma(i+1)}{\Gamma(i+\alpha+1)}\psi^{i+\alpha} \tag{4}$$

$$ {}^{RL}D^{\alpha}\psi^{i}=\frac{\Gamma(i+1)}{\Gamma(i-\alpha+1)}\psi^{i-\alpha} \tag{5}$$

Definition 3.

$$ I_{\psi}^{\alpha}\left({}^{RL}D_{\psi}^{\alpha}\right)f(\psi)=f(\psi)-\sum_{j=0}^{n}f^{j}(0)\frac{\psi^{j}}{j!}, \tag{6}$$

for $\psi > 0$, and $i-1 < \alpha \le i, i \in N$

$$\left({}^{RL}D_{\psi}^{\alpha}\right)I_{\psi}^{\alpha} f(\psi) = f(\psi) \tag{7}$$

Definition 4. The Caputo fractional operator ${}^{c}D^{\alpha}$ of order α is defined as follows [39, 40]:

$$ {}^{c}D^{\alpha}u(\psi) = \begin{cases} \dfrac{d^i}{d\psi^i}u(\psi), \alpha = i \\ \dfrac{1}{\Gamma(i-\psi)}\displaystyle\int_0^{\alpha} \dfrac{u^i(\psi)}{(\psi-\rho)^{\alpha-i+1}} d\psi, i-1 < \alpha < i \end{cases} \tag{8}$$

Definition 5. The fractional-order Caputo operator of the Elzaki transform is given as follows [39, 40]:

$$E\left[{}^{c}D_{\psi}^{\alpha} f(\psi)\right] = S^{-\alpha}E[f(\psi)] - \sum_{j=0}^{i-l} S^{2-\alpha+j} f^{(j)}(0), \tag{9}$$

for $i-1 < \alpha < i$.

THE GENERAL APPROACH OF THE ELZAKI PROJECTED DIFFERENTIAL TRANSFORM METHOD (EPDTM)

Let's explore the typical structure of a fractional partial differential equation,

$${}^{c}D_{\theta}^{\alpha}u(\psi,\theta) + Pu(\psi,\theta) + Qu(\psi,\theta) = g(\psi,\theta), \; i-1 < \alpha \le i, i \in N \tag{10}$$

where P and Q denote the linear and nonlinear operators, respectively, and g represents a source function. The initial condition can be stated as

$$u^{(l)}(\psi,0) = h_l(\psi), \; L = 0,1,2,\ldots,i-1, \tag{11}$$

Transforming Equation (10) using the the Elzaki transformation yields:

$$E\left[{}^{c}D_{\theta}^{\alpha}u(\psi,\theta)\right] + E[Pu(\psi,\theta) + Qu(\psi,\theta)] = E[g(\psi,\theta)] \tag{12}$$

Applying the Elzaki differentiation yields:

$$E[u(\psi,\theta)] = \sum_{j=0}^{n} S^{2-\alpha+j}u^{(j)}(\psi,0) + S^{\alpha}E[g(\psi,\theta)] - S^{\alpha}E[Pu(\psi,\theta) + Qu(\psi,\theta)], \tag{13}$$

The inverse Elzaki transform converts Equation (13) to:

$$u(\psi,\theta) = E^{-1}\left[\sum_{j=0}^{n} S^{2-\alpha+j}u^{(j)}(\psi,0) + S^{\alpha}E[g(\psi,\theta)]\right] - E^{-1}\left[S^{\alpha}E[Pu(\psi,\theta) + Qu(\psi,\theta)]\right] \tag{14}$$

Through the projected differential transform technique, we have

$$u(\psi,\theta) = \sum_{k=0}^{\infty} u_k(\psi,\theta) \tag{15}$$

Given the linearity of operator P and the nonlinearity of Operator Q, we observe the following outcome:

$$u_0(\psi,\theta) = E^{-1}\left[\sum_{j=0}^{n} S^{2-\alpha+j}u^{(j)}(\psi,0) + S^{\alpha}E[g(\psi,\theta)]\right], \tag{16}$$

$$u_1(\psi,\theta) = -E^{-1}\left[S^{\alpha} E\left[P u_0(\psi,\theta) + Q u_0(\psi,\theta)\right]\right], \tag{17}$$

$$u_{n+1}(\psi,\theta) = -E^{-1}\left[S^{\alpha} E\left[P\sum_{j=0}^{\infty} u_j(\psi,\theta) + Q\sum_{j=0}^{\infty} u_j(\psi,\theta)\right]\right], n \geq 1 \tag{18}$$

Ultimately, this produces the n-term result in series format, represented as:

$$u(\psi,\theta) = u_0(\psi,\theta) + u_1(\psi,\theta) + u_2(\psi,\theta) + u_3(\psi,\theta) + \ldots + u_n(\psi,\theta) \tag{19}$$

The resulting series solution $u(\psi,\theta) = \sum_{k=0}^{\infty} u_k(\psi,\theta)$ represents a time-domain reconstruction of the physical system's state, where each coefficient $u_k(\psi,\theta)$ captures the spatial behavior associated with the k-th time derivative of the solution. These coefficients are computed recursively using the EPDTM framework and encode how wave features like amplitude, dispersion, and nonlinearity evolve over time. In physical terms, the convergence of this series ensures that the computed solution accurately reflects the underlying wave dynamics governed by the fractional KdV system.

APPLICATIONS OF THE PROPOSED METHODOLOGY (EPDTM)

To demonstrate the effectiveness and simplicity of the method, several cases concerning fractional-order nonlinear systems of partial differential equations will be examined.

Case 1: Consider the fractional-order nonlinear Korteweg-de Vries (KdV) system, given by:

$$\frac{\partial^{\alpha} u}{\partial \theta^{\alpha}} = -c\frac{\partial^3 u}{\partial \psi^3} - 6cu\frac{\partial u}{\partial \psi} + 6v\frac{\partial v}{\partial \psi}, \quad 0 < \alpha < 1 \tag{20}$$

$$\frac{\partial^{\alpha} v}{\partial \theta^{\alpha}} = -c\frac{\partial^3 v}{\partial \psi^3} - 3cu\frac{\partial v}{\partial \psi},$$

with initial conditions

$$u(\psi,0) = \beta^2 \sec h^2\left(\frac{\varphi}{2} + \frac{\beta\psi}{2}\right), \quad v(\psi,0) = \sqrt{\frac{c}{2}}\beta^2 \sec h^2\left(\frac{\varphi}{2} + \frac{\beta\psi}{2}\right). \tag{21}$$

For $\alpha = 1$ the exact solutions of Equation (20) from the Korteweg-de Vries scheme are provided as follows:

$$u(\psi,\theta) = \beta^2 \sec h^2\left(\frac{\varphi}{2} + \frac{\beta\psi}{2} - \frac{c\beta^3\theta}{2}\right) \tag{22}$$

$$v(\psi,\theta) = \sqrt{\frac{c}{2}}\beta^2 \sec h^2\left(\frac{\varphi}{2} + \frac{\beta\psi}{2} - \frac{c\beta^3\theta}{2}\right)$$

Applying the Elzaki transform to Equation (20), we derive:

$$\frac{1}{S^{\alpha}} E[u(\psi,\theta)] - \sum_{j=0}^{n-1} S^{2-\alpha+j} u_{(j)}(\psi,0) = E\left[-c\frac{\partial^3 u}{\partial \psi^3} - 6cu\frac{\partial u}{\partial \psi} + 6v\frac{\partial v}{\partial \psi}\right] \tag{23}$$

$$\frac{1}{S^{\alpha}} E[v(\psi,\theta)] - \sum_{j=0}^{n-1} S^{2-\alpha+j} v_{(j)}(\psi,0) = E\left[-c\frac{\partial^3 v}{\partial \psi^3} - 3cu\frac{\partial v}{\partial \psi}\right]$$

$$\frac{1}{S^{\alpha}}E[u(\psi,\theta)] = S^{2-\alpha}u_{(0)}(\psi,0) + E\left[-c\frac{\partial^3 u}{\partial\psi^3} - 6cu\frac{\partial u}{\partial\psi} + 6v\frac{\partial v}{\partial\psi}\right] \tag{24}$$

$$\frac{1}{S^{\alpha}}E[v(\psi,\theta)] = S^{2-\alpha}v_{(0)}(\psi,0) + E\left[-c\frac{\partial^3 v}{\partial\psi^3} - 3cu\frac{\partial v}{\partial\psi}\right]$$

$$E[u(\psi,\theta)] = S^{2}u_{(0)}(\psi,0) + S^{\alpha}E\left[-c\frac{\partial^3 u}{\partial\psi^3} - 6cu\frac{\partial u}{\partial\psi} + 6v\frac{\partial v}{\partial\psi}\right] \tag{25}$$

$$E[v(\psi,\theta)] = S^{2}v_{(0)}(\psi,0) + S^{\alpha}E\left[-c\frac{\partial^3 v}{\partial\psi^3} - 3cu\frac{\partial v}{\partial\psi}\right]$$

By applying the inverse Elzaki transform to Equation (25), we obtain:

$$u(\psi,\theta) = E^{-1}\left[S^2 u_0(\psi,\theta)\right] + E^{-1}\left[S^{\alpha}E\left[-c\frac{\partial^3 u}{\partial\psi^3} - 6cu\frac{\partial u}{\partial\psi} + 6v\frac{\partial v}{\partial\psi}\right]\right] \tag{26}$$

$$v(\psi,\theta) = E^{-1}\left[S^2 v_0(\psi,\theta)\right] + E^{-1}\left[S^{\alpha}E\left[-c\frac{\partial^3 v}{\partial\psi^3} - 3cu\frac{\partial v}{\partial\psi}\right]\right],$$

And $u_0(\psi,\theta) = \beta^2 \operatorname{sech}^2\left(\frac{\varphi}{2} + \frac{\beta\psi}{2}\right)$, $v_0(\psi,0) = \sqrt{\frac{c}{2}}\beta^2 \operatorname{sech}^2\left(\frac{\varphi}{2} + \frac{\beta\psi}{2}\right)$

Now, employing the projected differential transform method, we obtain:

$$u_{n+1}(\psi,\theta) = E^{-1}\left[S^{\alpha}E\left[A_{n+1} + B_{n+1} + C_{n+1}\right]\right] \tag{27}$$

$$v_{n+1}(\psi,\theta) = E^{-1}\left[S^{\alpha}E\left[D_{n+1} + E_{n+1}\right]\right]$$

Where,

$$A_{n+1} = -c\frac{\partial^3 u_n(\psi,\theta)}{\partial\psi^3} \tag{28}$$

$$B_{n+1} = -6c\sum_{n=0}^{m} u_n(\psi,\theta)\frac{\partial u_{m-n}(\psi,\theta)}{\partial\psi}$$

$$C_{n+1} = 6\sum_{n=0}^{m} v_n(\psi,\theta)\frac{\partial v_{m-n}(\psi,\theta)}{\partial\psi}$$

$$D_{n+1} = -c\frac{\partial^3 v_n(\psi,\theta)}{\partial\psi^3}$$

$$E_{n+1} = -3c\sum_{n=0}^{m} u_n(\psi,\theta)\frac{\partial v_{m-n}(\psi,\theta)}{\partial\psi}$$

At n=0, we have,

$$u_1(\psi,\theta) = E^{-1}\left[S^{\alpha}E\left[A_1 + B_1 + C_1\right]\right] \tag{29}$$

$$v_1(\psi,\theta) = E^{-1}\left[S^{\alpha}E\left[D_1 + E_1\right]\right]$$

$$u_1(\psi,\theta)=E^{-1}\left[S^{\alpha}E\left[-c\frac{\partial^3 u_0(\psi,\theta)}{\partial\psi^3}+-6c\left(u_0(\psi,\theta)\frac{\partial u_0(\psi,\theta)}{\partial\psi}\right)+6\left(v_n(\psi,\theta)\frac{\partial v_{m-n}(\psi,\theta)}{\partial\psi}\right)\right]\right] \tag{30}$$

$$v_1(\psi,\theta)=E^{-1}\left[S^{\alpha}E\left[-c\frac{\partial^3 v_0(\psi,\theta)}{\partial\psi^3}-3c\left(u_0(\psi,\theta)\frac{\partial v_0(\psi,\theta)}{\partial\psi}\right)\right]\right]$$

$$u_1(\psi,\theta)=E^{-1}\left[S^{\alpha}E\left[c\beta^5\tanh\left(\frac{\varphi}{2}+\frac{\beta\psi}{2}\right)\sec h^2\left(\frac{\varphi}{2}+\frac{\beta\psi}{2}\right)\right]\right] \tag{31}$$

$$v_1(\psi,\theta)=E^{-1}\left[S^{\alpha}E\left[\frac{\sqrt{2}}{2}c^{\frac{3}{2}}\beta^5\tanh\left(\frac{\varphi}{2}+\frac{\beta\psi}{2}\right)\sec h^2\left(\frac{\varphi}{2}+\frac{\beta\psi}{2}\right)\right]\right]$$

$$u_1(\psi,\theta)=c\beta^5\tanh\left(\frac{\varphi}{2}+\frac{\beta\psi}{2}\right)\sec h^2\left(\frac{\varphi}{2}+\frac{\beta\psi}{2}\right)\frac{\theta^{\alpha}}{\Gamma(\alpha+1)}, \tag{32}$$

$$v_1(\psi,\theta)=\frac{\sqrt{2}}{2}c^{\frac{3}{2}}\beta^5\tanh\left(\frac{\varphi}{2}+\frac{\beta\psi}{2}\right)\sec h^2\left(\frac{\varphi}{2}+\frac{\beta\psi}{2}\right)\frac{\theta^{\alpha}}{\Gamma(\alpha+1)}.$$

At n = 1, we have

$$u_2(\psi,\theta)=E^{-1}\left[S^{\alpha}E[A_2+B_2+C_2]\right] \tag{33}$$

$$v_2(\psi,\theta)=E^{-1}\left[S^{\alpha}E[D_2+E_2]\right]$$

$$A_2=-c\frac{\partial^3 u_1(\psi,\theta)}{\partial\psi^3} \tag{34}$$

$$B_2=-6c\left(u_0(\psi,\theta)\frac{\partial u_1(\psi,\theta)}{\partial\psi}+u_1(\psi,\theta)\frac{\partial u_0(\psi,\theta)}{\partial\psi}\right)$$

$$C_2=6\left(v_0(\psi,\theta)\frac{\partial v_1(\psi,\theta)}{\partial\psi}+v_1(\psi,\theta)\frac{\partial v_0(\psi,\theta)}{\partial\psi}\right)$$

$$D_2=-c\frac{\partial^3 v_1(\psi,\theta)}{\partial\psi^3}$$

$$E_2=-3c\left(u_0(\psi,\theta)\frac{\partial v_1(\psi,\theta)}{\partial\psi}+u_1(\psi,\theta)\frac{\partial v_0(\psi,\theta)}{\partial\psi}\right)$$

$$u_2(\psi,\theta)=E^{-1}\left[S^{\alpha}E\left[\frac{c^2\beta^8}{2}\left(2\cosh^2\left(\frac{\varphi}{2}+\frac{\beta\psi}{2}\right)-3\right)\sec h^4\left(\frac{\varphi}{2}+\frac{\beta\psi}{2}\right)\frac{\theta^{\alpha}}{\Gamma(\alpha+1)}\right]\right] \tag{35}$$

$$v_2(\psi,\theta)=E^{-1}\left[S^{\alpha}E\left[\frac{\sqrt{2}}{4}c^{\frac{5}{2}}\beta^8\left(2\cosh^2\left(\frac{\varphi}{2}+\frac{\beta\psi}{2}\right)-3\right)\sec h^4\left(\frac{\varphi}{2}+\frac{\beta\psi}{2}\right)\frac{\theta^{\alpha}}{\Gamma(\alpha+1)}\right]\right]$$

$$u_2(\psi,\theta)=\frac{c^2\beta^8}{2}\left(2\cosh^2\left(\frac{\varphi}{2}+\frac{\beta\psi}{2}\right)-3\right)\sec h^4\left(\frac{\varphi}{2}+\frac{\beta\psi}{2}\right)\frac{\theta^{2\alpha}}{\Gamma(2\alpha+1)} \tag{36}$$

$$v_2(\psi,\theta)=\frac{\sqrt{2}}{4}c^{\frac{5}{2}}\beta^8\left(2\cosh^2\left(\frac{\varphi}{2}+\frac{\beta\psi}{2}\right)-3\right)\sec h^4\left(\frac{\varphi}{2}+\frac{\beta\psi}{2}\right)\frac{\theta^{2\alpha}}{\Gamma(2\alpha+1)}$$

At n = 2, we have

$$u_3(\psi,\theta)=E^{-1}\left[S^{\alpha}E\left[A_3+B_3+C_3\right]\right] \quad (37)$$

$$v_3(\psi,\theta)=E^{-1}\left[S^{\alpha}E\left[D_3+E_3\right]\right]$$

$$A_3=-c\frac{\partial^3 u_2(\psi,\theta)}{\partial\psi^3} \quad (38)$$

$$B_3=-6c\left(u_1(\psi,\theta)\frac{\partial u_2(\psi,\theta)}{\partial\psi}+u_2(\psi,\theta)\frac{\partial u_1(\psi,\theta)}{\partial\psi}\right)$$

$$C_3=6\left(v_1(\psi,\theta)\frac{\partial v_2(\psi,\theta)}{\partial\psi}+v_2(\psi,\theta)\frac{\partial v_1(\psi,\theta)}{\partial\psi}\right)$$

$$D_3=-c\frac{\partial^3 v_2(\psi,\theta)}{\partial\psi^3}$$

$$E_3=-3c\left(u_1(\psi,\theta)\frac{\partial v_2(\psi,\theta)}{\partial\psi}+u_2(\psi,\theta)\frac{\partial v_1(\psi,\theta)}{\partial\psi}\right)$$

$$u_3(\psi,\theta)=E^{-1}\left[S^{\alpha}E\left[-c\frac{\partial^3 u_2(\psi,\theta)}{\partial\psi^3}-6c\left(u_1(\psi,\theta)\frac{\partial u_2(\psi,\theta)}{\partial\psi}+u_2(\psi,\theta)\frac{\partial u_1(\psi,\theta)}{\partial\psi}\right)+6\left(v_1(\psi,\theta)\frac{\partial v_2(\psi,\theta)}{\partial\psi}+v_2(\psi,\theta)\frac{\partial v_1(\psi,\theta)}{\partial\psi}\right)\right]\right] \quad (39)$$

$$v_3(\psi,\theta)=E^{-1}\left[S^{\alpha}E\left[-c\frac{\partial^3 v_2(\psi,\theta)}{\partial\psi^3}-3c\left(u_1(\psi,\theta)\frac{\partial v_2(\psi,\theta)}{\partial\psi}+u_2(\psi,\theta)\frac{\partial v_1(\psi,\theta)}{\partial\psi}\right)\right]\right]$$

$$u_3(\psi,\theta)=\frac{\sec h^8\left(\frac{\varphi}{2}+\frac{\beta\psi}{2}\right)c^3\beta^{11}\theta^{3\alpha}}{4\Gamma(3\alpha+1)}\left[\begin{array}{l}\sinh\left(\frac{\varphi}{2}+\frac{\beta\psi}{2}\right)\left(\begin{array}{l}4\cosh^5\left(\frac{\varphi}{2}+\frac{\beta\psi}{2}\right)-60\sinh\left(\frac{\varphi}{2}+\frac{\beta\psi}{2}\right)\cosh^3\left(\frac{\varphi}{2}+\frac{\beta\psi}{2}\right)\\+90\sinh\left(\frac{\varphi}{2}+\frac{\beta\psi}{2}\right)\cosh\left(\frac{\varphi}{2}+\frac{\beta\psi}{2}\right)\end{array}\right)\\+\frac{c\beta^3\theta^{2\alpha}}{\Gamma(2\alpha+1)}\left(24\cosh^4\left(\frac{\varphi}{2}+\frac{\beta\psi}{2}\right)-84c\beta^3\cosh^2\left(\frac{\varphi}{2}+\frac{\beta\psi}{2}\right)+63\right)\end{array}\right] \quad (40)$$

$$v_3(\psi,\theta)=\frac{\sec h^8\left(\frac{\varphi}{2}+\frac{\beta\psi}{2}\right)c^{\frac{7}{2}}\beta^{11}\theta^{3\alpha}}{8\Gamma(3\alpha+1)}\left[\begin{array}{l}\sinh\left(\frac{\varphi}{2}+\frac{\beta\psi}{2}\right)\left(\begin{array}{l}4\cosh^5\left(\frac{\varphi}{2}+\frac{\beta\psi}{2}\right)-60\sinh\left(\frac{\varphi}{2}+\frac{\beta\psi}{2}\right)\cosh^3\left(\frac{\varphi}{2}+\frac{\beta\psi}{2}\right)\\+90\sinh\left(\frac{\varphi}{2}+\frac{\beta\psi}{2}\right)\cosh\left(\frac{\varphi}{2}+\frac{\beta\psi}{2}\right)\end{array}\right)\\+\frac{c\beta^3\theta^{2\alpha}}{\Gamma(2\alpha+1)}\left(24\cosh^4\left(\frac{\varphi}{2}+\frac{\beta\psi}{2}\right)-84c\beta^3\cosh^2\left(\frac{\varphi}{2}+\frac{\beta\psi}{2}\right)+63\right)\end{array}\right]$$

And so on, then the result in series form is given as

$$\begin{aligned}u(\psi,\theta)=&\ \beta^2\sec h^2\left(\frac{\varphi}{2}+\frac{\beta\psi}{2}\right)+c\beta^5\tanh\left(\frac{\varphi}{2}+\frac{\beta\psi}{2}\right)\sec h^2\left(\frac{\varphi}{2}+\frac{\beta\psi}{2}\right)\frac{\theta^{\alpha}}{\Gamma(\alpha+1)}\\&+\frac{c^2\beta^8}{2}\left(2\cosh^2\left(\frac{\varphi}{2}+\frac{\beta\psi}{2}\right)-3\right)\sec h^4\left(\frac{\varphi}{2}+\frac{\beta\psi}{2}\right)\frac{\theta^{2\alpha}}{\Gamma(2\alpha+1)}\\&+\frac{\sec h^8\left(\frac{\varphi}{2}+\frac{\beta\psi}{2}\right)c^3\beta^{11}\theta^{3\alpha}}{4\Gamma(3\alpha+1)}\left[\begin{array}{l}\sinh\left(\frac{\varphi}{2}+\frac{\beta\psi}{2}\right)\left(\begin{array}{l}4\cosh^5\left(\frac{\varphi}{2}+\frac{\beta\psi}{2}\right)-60\sinh\left(\frac{\varphi}{2}+\frac{\beta\psi}{2}\right)\cosh^3\left(\frac{\varphi}{2}+\frac{\beta\psi}{2}\right)\\+90\sinh\left(\frac{\varphi}{2}+\frac{\beta\psi}{2}\right)\cosh\left(\frac{\varphi}{2}+\frac{\beta\psi}{2}\right)\end{array}\right)\\+\frac{c\beta^3\theta^{2\alpha}}{\Gamma(2\alpha+1)}\left(24\cosh^4\left(\frac{\varphi}{2}+\frac{\beta\psi}{2}\right)-84c\beta^3\cosh^2\left(\frac{\varphi}{2}+\frac{\beta\psi}{2}\right)+63\right)\end{array}\right]+\ldots\end{aligned} \quad (41)$$

$$v(\psi,\theta)=\sqrt{\frac{c}{2}}\beta^2\sec h^2\left(\frac{\varphi}{2}+\frac{\beta\psi}{2}\right)+\frac{\sqrt{2}}{2}c^{\frac{3}{2}}\beta^5\tanh\left(\frac{\varphi}{2}+\frac{\beta\psi}{2}\right)\sec h^2\left(\frac{\varphi}{2}+\frac{\beta\psi}{2}\right)\frac{\theta^\alpha}{\Gamma(\alpha+1)} \quad (42)$$

$$+\frac{\sqrt{2}}{4}c^{\frac{5}{2}}\beta^8\left(2\cosh^2\left(\frac{\varphi}{2}+\frac{\beta\psi}{2}\right)-3\right)\sec h^4\left(\frac{\varphi}{2}+\frac{\beta\psi}{2}\right)\frac{\theta^{2\alpha}}{\Gamma(2\alpha+1)}$$

$$+\frac{\sec h^8\left(\frac{\varphi}{2}+\frac{\beta\psi}{2}\right)c^{\frac{7}{2}}\beta^{11}\theta^{3\alpha}}{8\Gamma(3\alpha+1)}\left[\begin{array}{l}\sinh\left(\frac{\varphi}{2}+\frac{\beta\psi}{2}\right)\left(\begin{array}{l}4\cosh^5\left(\frac{\varphi}{2}+\frac{\beta\psi}{2}\right)-60\sinh\left(\frac{\varphi}{2}+\frac{\beta\psi}{2}\right)\cosh^3\left(\frac{\varphi}{2}+\frac{\beta\psi}{2}\right)\\+90\sinh\left(\frac{\varphi}{2}+\frac{\beta\psi}{2}\right)\cosh\left(\frac{\varphi}{2}+\frac{\beta\psi}{2}\right)\end{array}\right)\\+\frac{c\beta^3\theta^{2\alpha}}{\Gamma(2\alpha+1)}\left(24\cosh^4\left(\frac{\varphi}{2}+\frac{\beta\psi}{2}\right)-84c\beta^3\cosh^2\left(\frac{\varphi}{2}+\frac{\beta\psi}{2}\right)+63\right)\end{array}\right]+\ldots$$

Case 2: Consider the fractional-order nonlinear Korteweg-de Vries (KdV) system, given by:

$$\frac{\partial^\alpha u}{\partial\theta^\alpha}=-\frac{\partial v}{\partial\psi}-\frac{1}{2}\frac{\partial u^2}{\partial\psi}, \qquad 0<\alpha<1 \quad (43)$$

$$\frac{\partial^\alpha v}{\partial\theta^\alpha}=-\frac{\partial u}{\partial\psi}-\frac{\partial^3 u}{\partial\psi^3}-\frac{\partial uv}{\partial\psi},$$

with initial conditions

$$u(\psi,0)=\beta\left(\tanh\left(\frac{\varphi}{2}+\frac{\beta\psi}{2}\right)+1\right), \quad v(\psi,0)=-1+\frac{1}{2}\beta^2\sec h^2\left(\frac{\varphi}{2}+\frac{\beta\psi}{2}\right). \quad (44)$$

For $\alpha=1$ the exact solutions of Equation (43) from the Korteweg-de Vries scheme are provided as follows:

$$u(\psi,\theta)=\beta\left(\tanh\left(\frac{\varphi}{2}+\frac{\beta\psi}{2}-\frac{\beta^2\psi}{2}\right)+1\right), \quad (45)$$

$$v(\psi,\theta)=-1+\frac{1}{2}\beta^2\sec h^2\left(\frac{\varphi}{2}+\frac{\beta\psi}{2}-\frac{\beta^2\psi}{2}\right).$$

Applying the Elzaki transform to Equation (43), we derive:

$$\frac{1}{S^\alpha}E[u(\psi,\theta)]-\sum_{j=0}^{n-1}S^{2-\alpha+j}u_{(j)}(\psi,0)=E\left[-\frac{\partial v}{\partial\psi}-\frac{1}{2}\frac{\partial u^2}{\partial\psi}\right] \quad (46)$$

$$\frac{1}{S^\alpha}E[v(\psi,\theta)]-\sum_{j=0}^{n-1}S^{2-\alpha+j}v_{(j)}(\psi,0)=E\left[-\frac{\partial u}{\partial\psi}-\frac{\partial^3 u}{\partial\psi^3}-\frac{\partial uv}{\partial\psi}\right]$$

$$\frac{1}{S^\alpha}E[u(\psi,\theta)]=S^{2-\alpha}u_{(0)}(\psi,0)+E\left[-\frac{\partial v}{\partial\psi}-\frac{1}{2}\frac{\partial u^2}{\partial\psi}\right] \quad (47)$$

$$\frac{1}{S^\alpha}E[v(\psi,\theta)]=S^{2-\alpha}v_{(0)}(\psi,0)+E\left[-\frac{\partial u}{\partial\psi}-\frac{\partial^3 u}{\partial\psi^3}-\frac{\partial uv}{\partial\psi}\right]$$

$$E[u(\psi,\theta)]=S^2u_{(0)}(\psi,0)+S^\alpha E\left[-\frac{\partial v}{\partial\psi}-\frac{1}{2}\frac{\partial u^2}{\partial\psi}\right] \quad (48)$$

$$E[v(\psi,\theta)]=S^2v_{(0)}(\psi,0)+S^\alpha E\left[-\frac{\partial u}{\partial\psi}-\frac{\partial^3 u}{\partial\psi^3}-\frac{\partial uv}{\partial\psi}\right]$$

By applying the inverse Elzaki transform to Equation (47), we obtain:

$$u(\psi,\theta)=E^{-1}\left[S^2u_{(0)}(\psi,0)\right]+E^{-1}\left[S^{\alpha}E\left[-\frac{\partial v}{\partial\psi}-\frac{1}{2}\frac{\partial u^2}{\partial\psi}\right]\right] \tag{49}$$

$$v(\psi,\theta)=E^{-1}\left[S^2v_{(0)}(\psi,0)\right]+E^{-1}\left[S^{\alpha}E\left[-\frac{\partial u}{\partial\psi}-\frac{\partial^3u}{\partial\psi^3}-\frac{\partial uv}{\partial\psi}\right]\right],$$

And $u_0(\psi,\theta)=\beta\left(\tanh\left(\frac{\varphi}{2}+\frac{\beta\psi}{2}\right)+1\right)$, $v_0(\psi,\theta)=-1+\frac{1}{2}\beta^2\sec h^2\left(\frac{\varphi}{2}+\frac{\beta\psi}{2}\right)$

Now, employing the projected differential transform method, we obtain:

$$u_{n+1}(\psi,\theta)=E^{-1}\left[S^{\alpha}E[A_{n+1}+B_{n+1}]\right] \tag{50}$$

$$v_{n+1}(\psi,\theta)=E^{-1}\left[S^{\alpha}E[C_{n+1}+D_{n+1}+E_{n+1}]\right]$$

Where,

$$A_{n+1}=-\frac{\partial v_n(\psi,\theta)}{\partial\psi}$$

$$B_{n+1}=-\frac{1}{2}\frac{\partial}{\partial\psi}\sum_{n=0}^{m}u_n(\psi,\theta)u_{m-n}(\psi,\theta) \tag{51}$$

$$C_{n+1}=-\frac{\partial u_n(\psi,\theta)}{\partial\psi}$$

$$D_{n+1}=-\frac{\partial^3u_n(\psi,\theta)}{\partial\psi^3}$$

$$E_{n+1}=-\frac{\partial}{\partial\psi}\sum_{n=0}^{m}u_n(\psi,\theta)v_{m-n}(\psi,\theta)$$

At n=0, we have,

$$u_1(\psi,\theta)=E^{-1}\left[S^{\alpha}E[A_1+B_1]\right] \tag{52}$$

$$v_1(\psi,\theta)=E^{-1}\left[S^{\alpha}E[C_1+D_1+E_1]\right]$$

$$u_1(\psi,\theta)=E^{-1}\left[S^{\alpha}E\left[-\frac{\partial v_0(\psi,\theta)}{\partial\psi}-\frac{1}{2}\left(\frac{\partial u_0(\psi,\theta)^2}{\partial\psi}\right)\right]\right] \tag{53}$$

$$v_1(\psi,\theta)=E^{-1}\left[S^{\alpha}E\left[-\frac{\partial u_0(\psi,\theta)}{\partial\psi}-\frac{\partial^3u_0(\psi,\theta)}{\partial\psi^3}-\frac{\partial u_0(\psi,\theta)v_0(\psi,\theta)}{\partial\psi}\right]\right]$$

$$u_1(\psi,\theta)=E^{-1}\left[S^{\alpha}E\left[-\frac{1}{2}\beta^3\sec h^2\left(\frac{\varphi}{2}+\frac{\beta\psi}{2}\right)\right]\right] \tag{54}$$

$$v_1(\psi,\theta)=E^{-1}\left[S^{\alpha}E\left[\frac{1}{2}\beta^4\sinh\left(\frac{\varphi}{2}+\frac{\beta\psi}{2}\right)\sec h^3\left(\frac{\varphi}{2}+\frac{\beta\psi}{2}\right)\right]\right]$$

$$u_1(\psi,\theta)=-\frac{1}{2}\beta^3\sec h^2\left(\frac{\varphi}{2}+\frac{\beta\psi}{2}\right)\frac{\theta^{\alpha}}{\Gamma(\alpha+1)}, \tag{55}$$

$$v_1(\psi,\theta)=\frac{1}{2}\beta^4\sinh\left(\frac{\varphi}{2}+\frac{\beta\psi}{2}\right)\sec h^3\left(\frac{\varphi}{2}+\frac{\beta\psi}{2}\right)\frac{\theta^{\alpha}}{\Gamma(\alpha+1)}.$$

At n = 1, we have

$$u_2(\psi,\theta)=E^{-1}\left[S^{\alpha}E[A_2+B_2]\right] \tag{56}$$

$$v_2(\psi,\theta)=E^{-1}\left[S^{\alpha}E[C_2+D_2+E_2]\right]$$

$$A_2=-\frac{\partial v_1(\psi,\theta)}{\partial\psi}$$

$$B_2=-\frac{1}{2}\frac{\partial}{\partial\psi}\left[u_0(\psi,\theta)u_1(\psi,\theta)+u_1(\psi,\theta)u_0(\psi,\theta)\right] \tag{57}$$

$$C_2=-\frac{\partial u_1(\psi,\theta)}{\partial\psi}$$

$$D_2=-\frac{\partial^3 u_1(\psi,\theta)}{\partial\psi^3}$$

$$E_2=-\frac{\partial}{\partial\psi}\left[u_0(\psi,\theta)v_1(\psi,\theta)+u_1(\psi,\theta)v_0(\psi,\theta)\right]$$

$$u_2(\psi,\theta)=E^{-1}\left[S^{\alpha}E\left[-\frac{\beta^5}{2}\sinh\left(\frac{\varphi}{2}+\frac{\beta\psi}{2}\right)\sec h^3\left(\frac{\varphi}{2}+\frac{\beta\psi}{2}\right)\frac{\theta^{\alpha}}{\Gamma(\alpha+1)}\right]\right] \tag{58}$$

$$v_2(\psi,\theta)=E^{-1}\left[S^{\alpha}E\left[\frac{\beta^6}{4}\left(2\cosh^2\left(\frac{\varphi}{2}+\frac{\beta\psi}{2}\right)-3\right)\sec h^4\left(\frac{\varphi}{2}+\frac{\beta\psi}{2}\right)\frac{\theta^{\alpha}}{\Gamma(\alpha+1)}\right]\right]$$

$$u_2(\psi,\theta)=-\frac{\beta^5}{2}\sinh\left(\frac{\varphi}{2}+\frac{\beta\psi}{2}\right)\sec h^3\left(\frac{\varphi}{2}+\frac{\beta\psi}{2}\right)\frac{\theta^{2\alpha}}{\Gamma(2\alpha+1)} \tag{59}$$

$$v_2(\psi,\theta)=\frac{1}{4}\beta^6\left(2\cosh^2\left(\frac{\varphi}{2}+\frac{\beta\psi}{2}\right)-3\right)\sec h^4\left(\frac{\varphi}{2}+\frac{\beta\psi}{2}\right)\frac{\theta^{2\alpha}}{\Gamma(2\alpha+1)}$$

At n = 2, we have

$$u_3(\psi,\theta)=E^{-1}\left[S^{\alpha}E[A_3+B_3]\right] \tag{60}$$

$$v_3(\psi,\theta)=E^{-1}\left[S^{\alpha}E[C_3+D_3+E_3]\right]$$

$$A_3=-\frac{\partial v_2(\psi,\theta)}{\partial\psi} \tag{61}$$

$$B_3=-\frac{1}{2}\frac{\partial}{\partial\psi}\left[u_1(\psi,\theta)u_2(\psi,\theta)+u_2(\psi,\theta)u_1(\psi,\theta)\right]$$

$$C_3=-\frac{\partial u_2(\psi,\theta)}{\partial\psi}$$

$$D_3=-\frac{\partial^3 u_2(\psi,\theta)}{\partial\psi^3}$$

$$E_3=-\frac{\partial}{\partial\psi}\left[u_1(\psi,\theta)v_2(\psi,\theta)+u_2(\psi,\theta)v_1(\psi,\theta)\right]$$

$$u_3(\psi,\theta)=\frac{\beta^7\theta^{3\alpha}}{8\Gamma(3\alpha+1)}\sec h^6\left(\frac{\varphi}{2}+\frac{\beta\psi}{2}\right)\left[\begin{array}{l}\left(4\sinh\left(\frac{\varphi}{2}+\frac{\beta\psi}{2}\right)\cosh^3\left(\frac{\varphi}{2}+\frac{\beta\psi}{2}\right)-12\sinh\left(\frac{\varphi}{2}+\frac{\beta\psi}{2}\right)\cosh\left(\frac{\varphi}{2}+\frac{\beta\psi}{2}\right)\right)\\+\left(4\cosh^2\left(\frac{\varphi}{2}+\frac{\beta\psi}{2}\right)-5\right)\frac{\beta^2\theta^{2\alpha}}{\Gamma(2\alpha+1)}\end{array}\right]$$

$$v_3(\psi,\theta) = -\frac{\beta^6}{8}\sec h^7\left(\frac{\varphi}{2}+\frac{\beta\psi}{2}\right)\left[\begin{array}{l}\left(\begin{array}{l}4\cosh^5\left(\frac{\varphi}{2}+\frac{\beta\psi}{2}\right)-6\cosh^3\left(\frac{\varphi}{2}+\frac{\beta\psi}{2}\right)+4\beta^2\cosh^5\left(\frac{\varphi}{2}+\frac{\beta\psi}{2}\right)\\ -30\beta^2\cosh^3\left(\frac{\varphi}{2}+\frac{\beta\psi}{2}\right)+30\beta^2\cosh\left(\frac{\varphi}{2}+\frac{\beta\psi}{2}\right)\end{array}\right)\frac{\theta^{3\alpha}}{\Gamma(3\alpha+1)}\\ +\left(8\cosh^2\left(\frac{\varphi}{2}+\frac{\beta\psi}{2}\right)\sinh\left(\frac{\varphi}{2}+\frac{\beta\psi}{2}\right)-15\sinh\left(\frac{\varphi}{2}+\frac{\beta\psi}{2}\right)\right)\frac{\beta^4\theta^{2\alpha}}{\Gamma(2\alpha+1)}\frac{\theta^{3\alpha}}{\Gamma(3\alpha+1)}\end{array}\right] \tag{62}$$

And so on, then the result in series form is given as

$$\begin{aligned}u(\psi,\theta) &= \beta\left(\tanh\left(\frac{\varphi}{2}+\frac{\beta\psi}{2}\right)+1\right)-\frac{1}{2}\beta^3\sec h^2\left(\frac{\varphi}{2}+\frac{\beta\psi}{2}\right)\frac{\theta^\alpha}{\Gamma(\alpha+1)}\\ &-\frac{\beta^5}{2}\sinh\left(\frac{\varphi}{2}+\frac{\beta\psi}{2}\right)\sec h^3\left(\frac{\varphi}{2}+\frac{\beta\psi}{2}\right)\frac{\theta^{2\alpha}}{\Gamma(2\alpha+1)}\\ &+\frac{\beta^7\theta^{3\alpha}}{8\Gamma(3\alpha+1)}\sec h^6\left(\frac{\varphi}{2}+\frac{\beta\psi}{2}\right)\left[\begin{array}{l}\left(4\sinh\left(\frac{\varphi}{2}+\frac{\beta\psi}{2}\right)\cosh^3\left(\frac{\varphi}{2}+\frac{\beta\psi}{2}\right)-12\sinh\left(\frac{\varphi}{2}+\frac{\beta\psi}{2}\right)\cosh\left(\frac{\varphi}{2}+\frac{\beta\psi}{2}\right)\right)\\ +\left(4\cosh^2\left(\frac{\varphi}{2}+\frac{\beta\psi}{2}\right)-5\right)\frac{\beta^2\theta^{2\alpha}}{\Gamma(2\alpha+1)}\end{array}\right]+\ldots\end{aligned} \tag{63}$$

$$\begin{aligned}v(\psi,\theta) &= -1+\frac{1}{2}\beta^2\sec h^2\left(\frac{\varphi}{2}+\frac{\beta\psi}{2}\right)+\frac{1}{2}\beta^4\sinh\left(\frac{\varphi}{2}+\frac{\beta\psi}{2}\right)\sec h^3\left(\frac{\varphi}{2}+\frac{\beta\psi}{2}\right)\frac{\theta^\alpha}{\Gamma(\alpha+1)}\\ &\frac{1}{4}\beta^6\left(2\cosh^2\left(\frac{\varphi}{2}+\frac{\beta\psi}{2}\right)-3\right)\sec h^4\left(\frac{\varphi}{2}+\frac{\beta\psi}{2}\right)\frac{\theta^{2\alpha}}{\Gamma(2\alpha+1)}\\ &-\frac{\beta^6\theta^{3\alpha}}{8\Gamma(3\alpha+1)}\sec h^7\left(\frac{\varphi}{2}+\frac{\beta\psi}{2}\right)\left[\begin{array}{l}\left(\begin{array}{l}4\cosh^5\left(\frac{\varphi}{2}+\frac{\beta\psi}{2}\right)-6\cosh^3\left(\frac{\varphi}{2}+\frac{\beta\psi}{2}\right)+4\beta^2\cosh^5\left(\frac{\varphi}{2}+\frac{\beta\psi}{2}\right)\\ -30\beta^2\cosh^3\left(\frac{\varphi}{2}+\frac{\beta\psi}{2}\right)+30\beta^2\cosh\left(\frac{\varphi}{2}+\frac{\beta\psi}{2}\right)\end{array}\right)\\ +\left(8\cosh^2\left(\frac{\varphi}{2}+\frac{\beta\psi}{2}\right)\sinh\left(\frac{\varphi}{2}+\frac{\beta\psi}{2}\right)-15\sinh\left(\frac{\varphi}{2}+\frac{\beta\psi}{2}\right)\right)\frac{\beta^4\theta^{2\alpha}}{\Gamma(2\alpha+1)}\end{array}\right]+\ldots\end{aligned} \tag{64}$$

RESULTS AND DISCUSSION

In this section, we rigorously examined the outcomes derived from the EPDTM (Elzaki Projected Differential Method) for both Case 1 and Case 2. Our objective was to assess and verify the effectiveness, convergence, and accuracy of these methods by comparing them against exact solutions. This analysis aims to establish the validity of our approach and derive meaningful conclusions.

Case 1: We have the exaction solution to be $\begin{array}{l}u(\psi,\theta)=\beta^2\sec h^2\left(\frac{\varphi}{2}+\frac{\beta\psi}{2}-\frac{c\beta^3\theta}{2}\right)\\ v(\psi,\theta)=\sqrt{\frac{c}{2}}\beta^2\sec h^2\left(\frac{\varphi}{2}+\frac{\beta\psi}{2}-\frac{c\beta^3\theta}{2}\right)\end{array}$, and the numerical solution using EPDTM is given in equation (41) and (42) to be $\beta := 0.1;\ \alpha := 0.5;\ c := 5;\ \varphi := 0.1;\ \psi := -30;\ \theta := 0.1$

$$
\begin{aligned}
u(\psi,\theta) &= \beta^2 \operatorname{sech}^2\left(\frac{\varphi}{2}+\frac{\beta\psi}{2}\right) + c\beta^5 \tanh\left(\frac{\varphi}{2}+\frac{\beta\psi}{2}\right)\operatorname{sech}^2\left(\frac{\varphi}{2}+\frac{\beta\psi}{2}\right)\frac{\theta^\alpha}{\Gamma(\alpha+1)} \\
&+ \frac{c^2\beta^8}{2}\left(2\cosh^2\left(\frac{\varphi}{2}+\frac{\beta\psi}{2}\right)-3\right)\operatorname{sech}^4\left(\frac{\varphi}{2}+\frac{\beta\psi}{2}\right)\frac{\theta^{2\alpha}}{\Gamma(2\alpha+1)} \\
&+ \frac{\operatorname{sech}^8\left(\frac{\varphi}{2}+\frac{\beta\psi}{2}\right)c^3\beta^{11}\theta^{3\alpha}}{4\Gamma(3\alpha+1)}\left[\begin{array}{l}
\sinh\left(\frac{\varphi}{2}+\frac{\beta\psi}{2}\right)\left(\begin{array}{l}4\cosh^5\left(\frac{\varphi}{2}+\frac{\beta\psi}{2}\right)-60\sinh\left(\frac{\varphi}{2}+\frac{\beta\psi}{2}\right)\cosh^3\left(\frac{\varphi}{2}+\frac{\beta\psi}{2}\right) \\ +90\sinh\left(\frac{\varphi}{2}+\frac{\beta\psi}{2}\right)\cosh\left(\frac{\varphi}{2}+\frac{\beta\psi}{2}\right)\end{array}\right) \\
+\frac{c\beta^3\theta^{2\alpha}}{\Gamma(2\alpha+1)}\left(24\cosh^4\left(\frac{\varphi}{2}+\frac{\beta\psi}{2}\right)-84c\beta^3\cosh^2\left(\frac{\varphi}{2}+\frac{\beta\psi}{2}\right)+63\right)
\end{array}\right]+\ldots
\end{aligned}
$$

$$
\begin{aligned}
v(\psi,\theta) &= \sqrt{\frac{c}{2}}\beta^2 \operatorname{sech}^2\left(\frac{\varphi}{2}+\frac{\beta\psi}{2}\right) + \frac{\sqrt{2}}{2}c^{\frac{3}{2}}\beta^5 \tanh\left(\frac{\varphi}{2}+\frac{\beta\psi}{2}\right)\operatorname{sech}^2\left(\frac{\varphi}{2}+\frac{\beta\psi}{2}\right)\frac{\theta^\alpha}{\Gamma(\alpha+1)} \\
&+ \frac{\sqrt{2}}{4}c^{\frac{5}{2}}\beta^8\left(2\cosh^2\left(\frac{\varphi}{2}+\frac{\beta\psi}{2}\right)-3\right)\operatorname{sech}^4\left(\frac{\varphi}{2}+\frac{\beta\psi}{2}\right)\frac{\theta^{2\alpha}}{\Gamma(2\alpha+1)} \\
&+ \frac{\operatorname{sech}^8\left(\frac{\varphi}{2}+\frac{\beta\psi}{2}\right)c^{\frac{7}{2}}\beta^{11}\theta^{3\alpha}}{8\Gamma(3\alpha+1)}\left[\begin{array}{l}
\sinh\left(\frac{\varphi}{2}+\frac{\beta\psi}{2}\right)\left(\begin{array}{l}4\cosh^5\left(\frac{\varphi}{2}+\frac{\beta\psi}{2}\right)-60\sinh\left(\frac{\varphi}{2}+\frac{\beta\psi}{2}\right)\cosh^3\left(\frac{\varphi}{2}+\frac{\beta\psi}{2}\right) \\ +90\sinh\left(\frac{\varphi}{2}+\frac{\beta\psi}{2}\right)\cosh\left(\frac{\varphi}{2}+\frac{\beta\psi}{2}\right)\end{array}\right) \\
+\frac{c\beta^3\theta^{2\alpha}}{\Gamma(2\alpha+1)}\left(24\cosh^4\left(\frac{\varphi}{2}+\frac{\beta\psi}{2}\right)-84c\beta^3\cosh^2\left(\frac{\varphi}{2}+\frac{\beta\psi}{2}\right)+63\right)
\end{array}\right]+\ldots
\end{aligned}
$$

For case 1; at $\beta = 0.0001, c = 0.05, \varphi = 0.00001,$ and $\alpha = 1$. Figures 1 and 2 illustrate the graphical representation of the exact solutions for $u(\psi,\theta)$ and $v(\psi,\theta)$, respectively. Figures 1 and 2 present the solutions for $u(\psi,\theta)$ and $v(\psi,\theta)$ as obtained via the Elzaki Projected Differential Transform Method (EPDTM). Table 1 presents a comparative assessment of the convergence characteristics of fractional solutions obtained using EPDTM in relation to the corresponding integer-order solutions and exact solutions, emphasizing the method's accuracy and dependability at

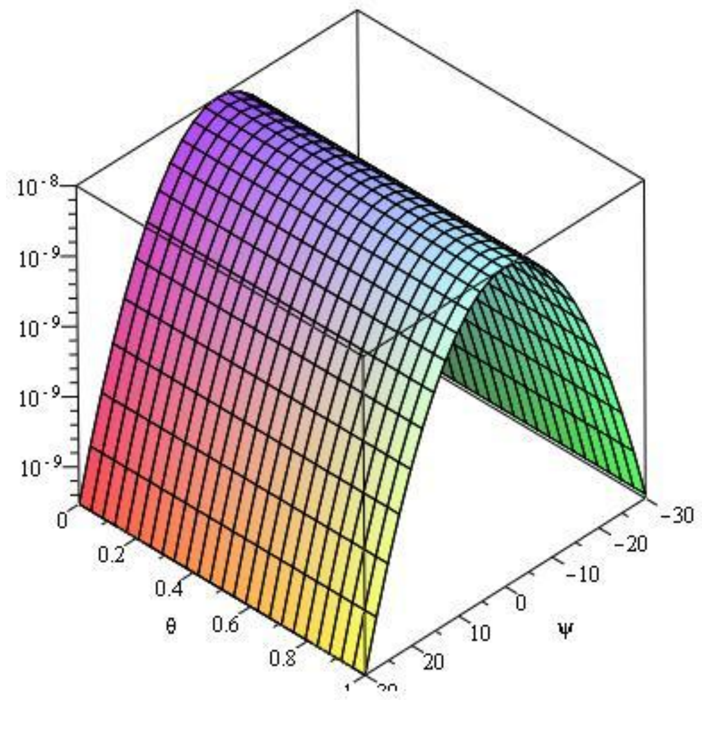

Figure 1. Exact analytical solution of the function $u(\psi,\theta)$ for Case 1 of the fractional KdV system. This plot serves as a reference benchmark for validating the numerical results obtained using EPDTM.

EDUCATUM JSMT Vol. 12 Number 1 (2026)
ISSN 2289-7070 / e-ISSN 2462-2451(1-23)
https://ejournal.upsi.edu.my/index.php/EJSMT/index

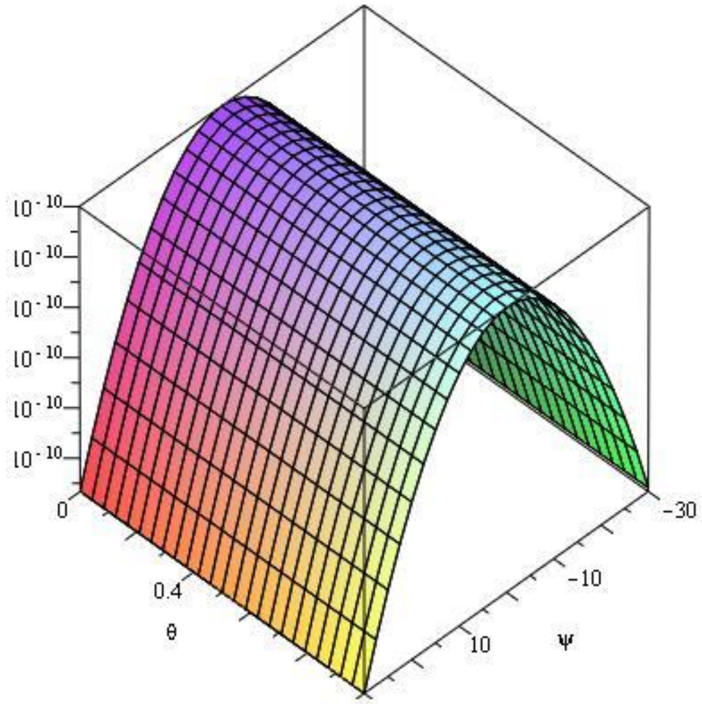

Figure 2. Exact analytical solution of the function $v(\psi,\theta)$ for Case 1. This result is used to assess the accuracy of the EPDTM in approximating the coupled system.

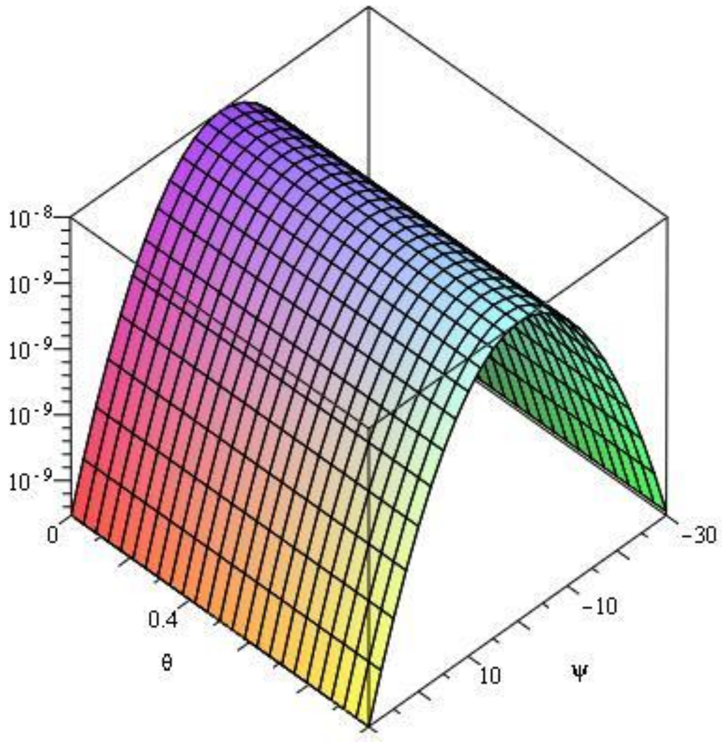

Figure 3. Numerical solution of $u(\psi,\theta)$ for Case 1 obtained using the Elzaki Projected Differential Transform Method (EPDTM). The solution closely approximates the exact profile shown in Figure 1.

EDUCATUM JSMT Vol. 12 Number 1 (2026)
ISSN 2289-7070 / e-ISSN 2462-2451(1-23)
https://ejournal.upsi.edu.my/index.php/EJSMT/index

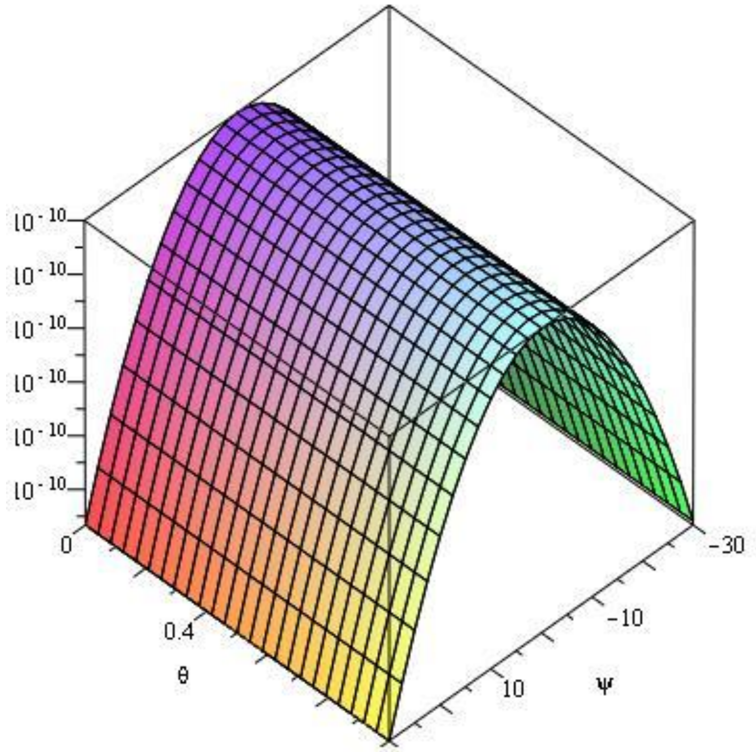

Figure 1. Numerical solution of $v(\psi, \theta)$ for Case 1 computed using EPDTM, matching the behavior of the exact solution in Figure 2.

Table 1. Comparative analysis of the convergence behaviour of the fractional solutions to the integer-order solutions through EPDTM with the exact solution for case 1

Case 1		$\alpha = 0.5$		**EPDTM (** $\alpha = 1$ **)**		**Exact (** $\alpha = 1$ **)**		**Error**	
ψ	θ	u	v	u	v	u	v	u	v
-30	0.1	0.001974186393	0.003121462761	0.001976457386	0.003125053519	0.001976457385	0.003125053517	0.000000000001	0.000000000002
	0.2	0.001972881029	0.003119398795	0.001975572361	0.003123654173	0.001975572361	0.003123654171	0.000000000000	0.000000000002
	0.3	0.001971880202	0.003117816342	0.001974687686	0.003122255377	0.001974687684	0.003122255374	0.000000000002	0.000000000003
	0.4	0.001971037018	0.003116483142	0.001973803359	0.003120857132	0.001973803354	0.003120857126	0.000000000005	0.000000000006
	0.5	0.001970294574	0.003115309228	0.001927919379	0.003119459438	0.001972919373	0.003119459429	0.000000000006	0.000000000008
0	0.1	0.009975918340	0.01577331185	0.009975290157	0.01577231861	0.009975290157	0.015772318610	0.000000000000	0.000000000000
	0.2	0.009976274262	0.01577387460	0.009975537471	0.01577270965	0.009975537469	0.015772709640	0.000000000002	0.000000000001
	0.3	0.009976544504	0.01577430187	0.009975783546	0.01577309872	0.009975783543	0.015773098720	0.000000000003	0.000000000000
	0.4	0.009976770396	0.01577465903	0.009976028388	0.01577348586	0.009976028379	0.015773485840	0.000000000009	0.000000000002
	0.5	0.009976967947	0.01577497137	0.009976271992	0.01577387102	0.009976271978	0.015773871000	0.000000000014	0.000000000002
30	0.1	0.001652653822	0.002613075133	0.001650714790	0.002610009252	0.001650714791	0.002610009253	0.000000000001	0.000000000001
	0.2	0.001653771130	0.002614841754	0.001651469111	0.002611201938	0.001651469111	0.002611201938	0.000000000000	0.000000000000
	0.3	0.001654629188	0.002616198469	0.001652223741	0.002612395113	0.001652223743	0.002612395116	0.000000000002	0.000000000003
	0.4	0.001655353049	0.002617342998	0.001652978681	0.002613588780	0.001652978685	0.002613588784	0.000000000004	0.000000000004
	0.5	0.001655991151	0.002618351930	0.001653733933	0.002614782936	0.001653733938	0.002614782944	0.000000000005	0.000000000008

Case 2: We have the exaction solution to be $u(\psi,\theta)=\beta\left(\tanh\left(\frac{\varphi}{2}+\frac{\beta\psi}{2}-\frac{\beta^2\psi}{2}\right)+1\right),\quad v(\psi,\theta)=-1+\frac{1}{2}\beta^2\sec h^2\left(\frac{\varphi}{2}+\frac{\beta\psi}{2}-\frac{\beta^2\psi}{2}\right).$, and the numerical solution using EPDTM is given in equation (63) and (64) to be

$$u(\psi,\theta)=\beta\left(\tanh\left(\frac{\varphi}{2}+\frac{\beta\psi}{2}\right)+1\right)-\frac{1}{2}\beta^3\sec h^2\left(\frac{\varphi}{2}+\frac{\beta\psi}{2}\right)\frac{\theta^\alpha}{\Gamma(\alpha+1)}$$
$$-\frac{\beta^5}{2}\sinh\left(\frac{\varphi}{2}+\frac{\beta\psi}{2}\right)\sec h^3\left(\frac{\varphi}{2}+\frac{\beta\psi}{2}\right)\frac{\theta^{2\alpha}}{\Gamma(2\alpha+1)}$$
$$+\frac{\beta^7\theta^{3\alpha}}{8\Gamma(3\alpha+1)}\sec h^6\left(\frac{\varphi}{2}+\frac{\beta\psi}{2}\right)\left[\begin{array}{l}\left(4\sinh\left(\frac{\varphi}{2}+\frac{\beta\psi}{2}\right)\cosh^3\left(\frac{\varphi}{2}+\frac{\beta\psi}{2}\right)-12\sinh\left(\frac{\varphi}{2}+\frac{\beta\psi}{2}\right)\cosh\left(\frac{\varphi}{2}+\frac{\beta\psi}{2}\right)\right)\\+\left(4\cosh^2\left(\frac{\varphi}{2}+\frac{\beta\psi}{2}\right)-5\right)\frac{\beta^2\theta^{2\alpha}}{\Gamma(2\alpha+1)}\end{array}\right]+\ldots$$

$$v(\psi,\theta)=-1+\frac{1}{2}\beta^2\sec h^2\left(\frac{\varphi}{2}+\frac{\beta\psi}{2}\right)+\frac{1}{2}\beta^4\sinh\left(\frac{\varphi}{2}+\frac{\beta\psi}{2}\right)\sec h^3\left(\frac{\varphi}{2}+\frac{\beta\psi}{2}\right)\frac{\theta^\alpha}{\Gamma(\alpha+1)}$$
$$\frac{1}{4}\beta^6\left(2\cosh^2\left(\frac{\varphi}{2}+\frac{\beta\psi}{2}\right)-3\right)\sec h^4\left(\frac{\varphi}{2}+\frac{\beta\psi}{2}\right)\frac{\theta^{2\alpha}}{\Gamma(2\alpha+1)}$$
$$-\frac{\beta^6\theta^{3\alpha}}{8\Gamma(3\alpha+1)}\sec h^7\left(\frac{\varphi}{2}+\frac{\beta\psi}{2}\right)\left[\begin{array}{l}\left(\begin{array}{l}4\cosh^5\left(\frac{\varphi}{2}+\frac{\beta\psi}{2}\right)-6\cosh^3\left(\frac{\varphi}{2}+\frac{\beta\psi}{2}\right)+4\beta^2\cosh^5\left(\frac{\varphi}{2}+\frac{\beta\psi}{2}\right)\\-30\beta^2\cosh^3\left(\frac{\varphi}{2}+\frac{\beta\psi}{2}\right)+30\beta^2\cosh\left(\frac{\varphi}{2}+\frac{\beta\psi}{2}\right)\end{array}\right)\\+\left(8\cosh^2\left(\frac{\varphi}{2}+\frac{\beta\psi}{2}\right)\sinh\left(\frac{\varphi}{2}+\frac{\beta\psi}{2}\right)-15\sinh\left(\frac{\varphi}{2}+\frac{\beta\psi}{2}\right)\right)\frac{\beta^4\theta^{2\alpha}}{\Gamma(2\alpha+1)}\end{array}\right]+\ldots$$

For case 2; at $\beta=0.1, c=5, \varphi=0.1,$ and $\alpha=1$. Figures 3 and 4 illustrate the graphical representation of the exact solutions for $u(\psi,\theta)$ and $v(\psi,\theta)$, respectively. Figures 3 and 4 present the solutions for $u(\psi,\theta)$ and $v(\psi,\theta)$ as obtained via the Elzaki Projected Differential Transform Method (EPDTM). Table 2 provides a comparative analysis of the convergence behavior of the fractional solutions derived through EPDTM relative to the exact solutions, highlighting the method's precision and reliability. $\psi=-30..30, \theta=0..1$

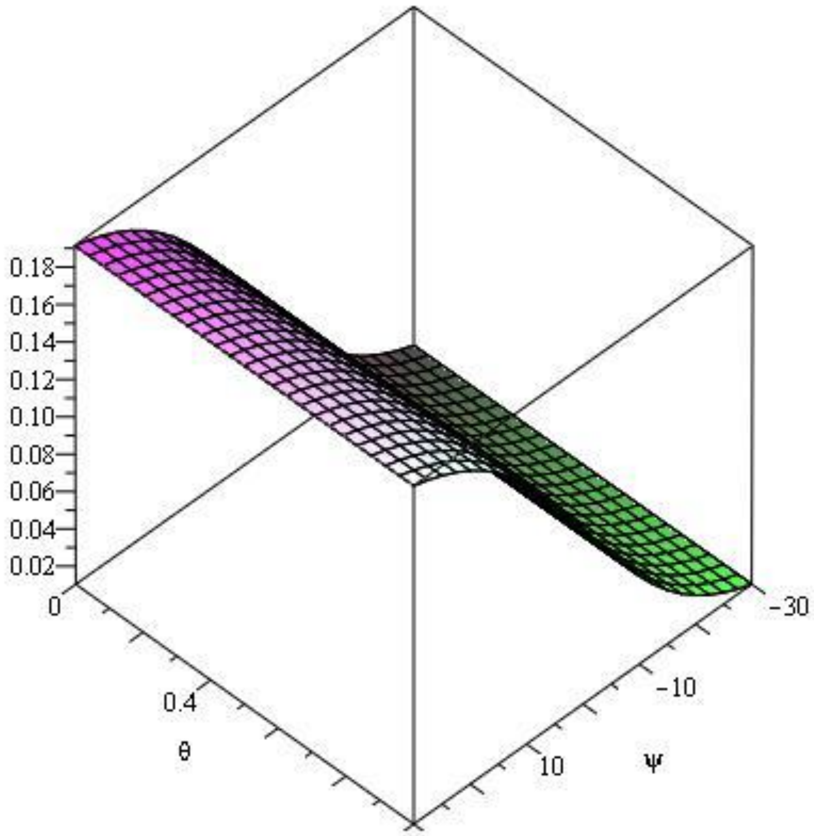

Figure 2. Exact analytical solution of $u(\psi, \theta)$ for Case 2 of the fractional KdV system. This reference solution enables a direct comparison with EPDTM-based numerical results.

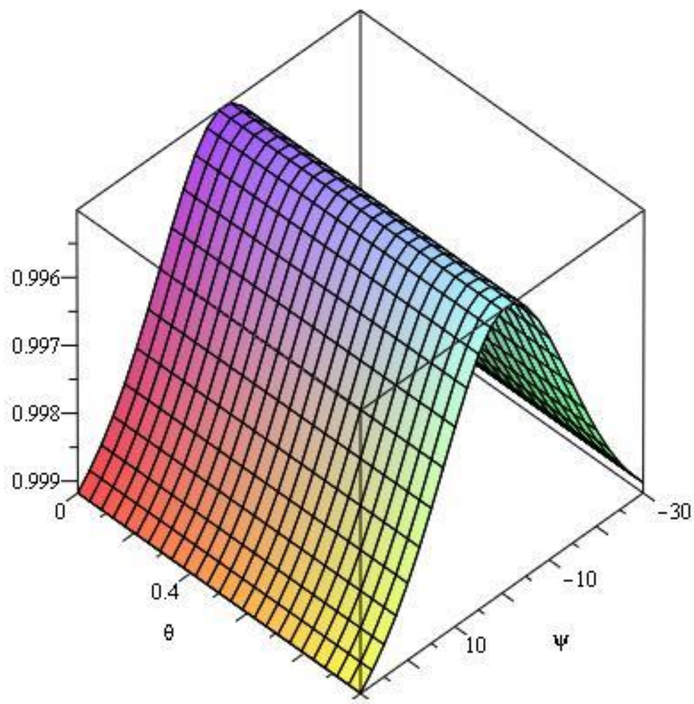

Figure 3. Exact analytical solution of $v(\psi, \theta)$ for Case 2. Used for validating the accuracy of the proposed EPDTM approach in solving the coupled system

EDUCATUM JSMT Vol. 12 Number 1 (2026)
ISSN 2289-7070 / e-ISSN 2462-2451(1-23)
https://ejournal.upsi.edu.my/index.php/EJSMT/index

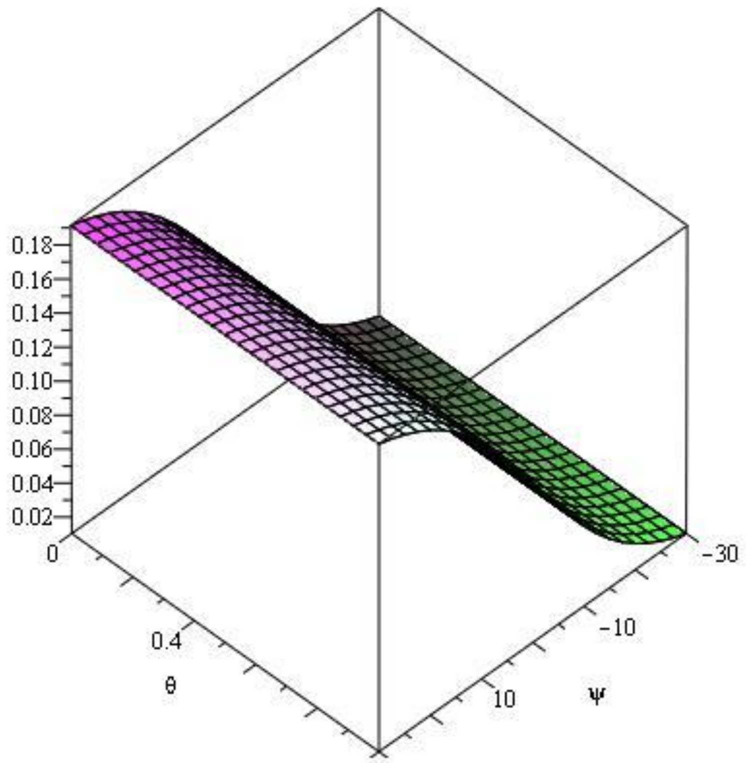

Figure 4. Numerical approximation of $u(\psi,\theta)$ for Case 2 using EPDTM. The result demonstrates strong agreement with the exact solution shown in Figure 5.

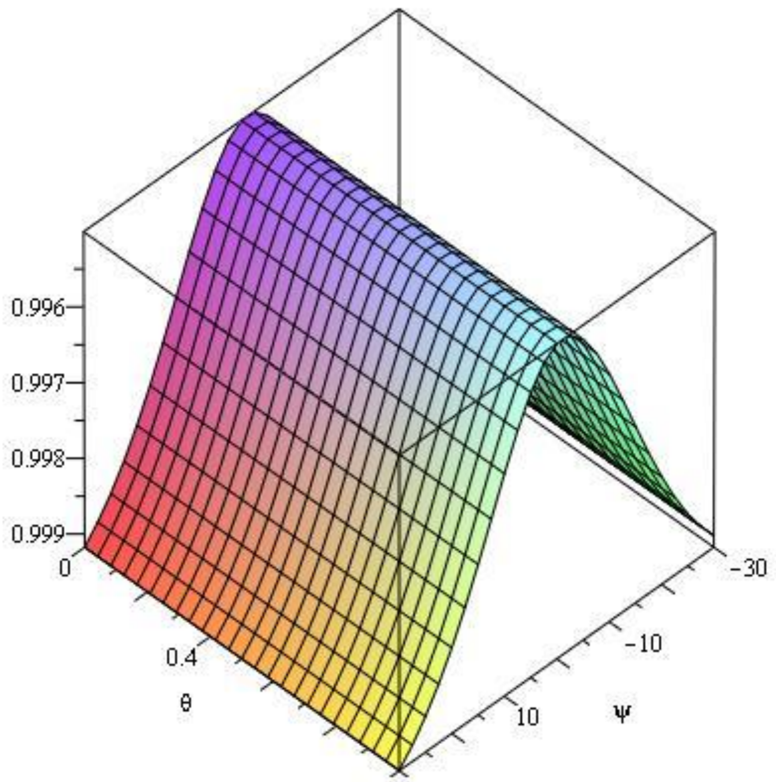

Figure 5. Numerical EPDTM solution for $v(\psi,\theta)$ in Case 2, exhibiting close alignment with the exact solution from Figure 6

Table 2. Comparative analysis of the convergence behaviour of the fractional solutions to the integer-order solutions through EPDTM with the exact solution for case 2

Case 1		$\alpha = 0.5$		EPDTM ($\alpha = 1$)		Exact ($\alpha = 1$)		Error	
ψ	θ	u	v	u	v	u	v	u	v
-30	0.1	0.01039552283	-0.9990144830	0.01042083034	-0.9990122138	0.01042083033	-0.9990122138	0.00000000000	0.00000000000
	0.2	0.01038099851	-0.9990157881	0.01041095690	-0.9990130984	0.01041095689	-0.9990130983	0.00000000001	0.00000000001
	0.3	0.01036987412	-0.9990167893	0.01040109231	-0.9990139824	0.01040109229	-0.9990139821	0.00000000002	0.00000000003
	0.4	0.01036050966	-0.9990176337	0.01039123656	-0.9990148659	0.01039123653	-0.9990148652	0.00000000003	0.00000000007
	0.5	0.01035226987	-0.9990183778	0.01038138966	-0.9990157490	0.01038138960	-0.9990157477	0.00000000006	0.00000000013
0	0.1	0.10481784540	-0.9950116091	0.10494596110	-0.9950122312	0.10494596100	-0.9950122313	0.00000000010	0.00000000001
	0.2	0.10474410390	-0.9950112550	0.10489608210	-0.9950119856	0.10489608210	-0.9950119858	0.00000000000	0.00000000002
	0.3	0.10468751400	-0.9950109835	0.10484620070	-0.9950117417	0.10484620080	-0.9950117428	0.00000000010	0.00000000011
	0.4	0.10463980260	-0.9950107538	0.10479631670	-0.9950114997	0.10479631700	-0.9950115023	0.00000000030	0.00000000006
	0.5	0.10459776500	-0.9950105504	0.10474643030	-0.9950112592	0.10474643080	-0.9950112643	0.00000000050	0.00000000051
30	0.1	0.19134903640	-0.9991723250	0.19137029540	-0.9991742654	0.19137029540	-0.9991742654	0.00000000000	0.00000000000
	0.2	0.19133676780	-0.9991712072	0.19136203430	-0.9991735108	0.19136203430	-0.9991735107	0.00000000000	0.00000000001
	0.3	0.19132733630	-0.9991703496	0.19135376570	-0.9991727555	0.19135376560	-0.9991727552	0.00000000010	0.00000000003
	0.4	0.19131937350	-0.9991696267	0.19134548950	-0.9991719999	0.19134548940	-0.9991719992	0.00000000010	0.00000000007
	0.5	0.19131234920	-0.9991689902	0.19133720590	-0.9991712438	0.19133720560	-0.9991712426	0.00000000030	0.00000000012

The error analysis presented in the tables reveals that the absolute error between the EPDTM solutions and the exact solutions remains consistently low across the spatial domain. Notably, at representative points such as x=−30, x=0, and x=30, the numerical results maintain high accuracy, with only minor variations due to the influence of fractional order dynamics. This demonstrates that EPDTM offers reliable spatial convergence and maintains solution fidelity throughout the domain, regardless of distance from the origin.

CONCLUSION

In this study, we explored the application of the Elzaki Projected Differential Transform Method (EPDTM) to fractional-order nonlinear Korteweg-de Vries (KdV) systems. Through detailed analysis and numerical simulations, we demonstrated the effectiveness and applicability of EPDTM in deriving approximate solutions for these complex systems. Firstly, we established the general approach of EPDTM for fractional partial differential equations, emphasizing its capability to handle both linear and nonlinear operators effectively. By applying the method to fractional-order KdV equations, we derived approximate solutions that closely approximate the exact solutions derived from theoretical frameworks. Specifically, we examined two illustrative cases of fractional-order nonlinear KdV systems. For each case, we conducted thorough numerical simulations and compared the results obtained through EPDTM with exact solutions. The comparison revealed excellent convergence and accuracy of EPDTM in capturing the behavior of fractional-order systems over time and space domains. Our findings underscore the utility of EPDTM in addressing challenges posed by fractional derivatives in nonlinear PDEs, offering a robust computational tool for researchers and practitioners in various fields of science and engineering. The method's ability to provide accurate approximations while maintaining computational efficiency makes it particularly valuable for studying complex physical phenomena governed by fractional-order dynamics.

In addition to its numerical accuracy, EPDTM exhibits significant computational efficiency. The method produces accurate approximations using only a few terms in the series expansion, avoiding the iterative correction steps commonly required by methods such as ADM or VIM. This reduction in computational effort translates into faster runtimes and lower memory usage, making EPDTM particularly suitable for large-scale or real-time simulations involving fractional-order systems. Looking ahead, further research could explore enhancements and extensions of EPDTM, such as incorporating adaptive techniques

or exploring its application to other classes of nonlinear PDEs. Such efforts would deepen our understanding and broaden the practical applications of EPDTM in modeling and analysis of complex systems.
In conclusion, this study contributes to advancing the methodology of solving fractional-order PDEs and provides a solid foundation for future explorations in this interdisciplinary field.

ACKNOWLEDGEMENT

Mrs. Oluwaremilekun Gbodogbe and my co-author are appreciated for their love and kind heartedness.

DECLARATION OF INTEREST

There is no conflict of interest with this study.

REFERENCES

[1]. Gardner, C. S., Greene, J. M., Kruskal, M. D., & Miura, R. M. (1967). Method for solving the Korteweg-deVries equation. Physical review letters, 19(19), 1095.

[2]. Jafari, H., Jassim, H. K., Baleanu, D., & Chu, Y. M. (2021). On the approximate solutions for a system of coupled Korteweg–de Vries equations with local fractional derivative. Fractals, 29(05), 2140012.

[3]. Park, C., Nuruddeen, R. I., Ali, K. K., Muhammad, L., Osman, M. S., & Baleanu, D. (2020). Novel hyperbolic and exponential ansatz methods to the fractional fifth-order Korteweg–de Vries equations. Advances in Difference Equations, 2020, 1-12.

[4]. Xiang, T. (2015). A summary of the Korteweg-de Vries equation. Institute for Mathematical Sciences, Renmin University of China, Beijing, 100872.

[5]. Korteweg, D. J., & De Vries, G. (1895). XLI. On the change of form of long waves advancing in a rectangular canal, and on a new type of long stationary waves. The London, Edinburgh, and Dublin Philosophical Magazine and Journal of Science, 39(240), 422-443.

[6]. Rizvi, S. T. R., Seadawy, A. R., Ashraf, F., Younis, M., Iqbal, H., & Baleanu, D. (2020). Lump and interaction solutions of a geophysical Korteweg–de Vries equation. Results in Physics, 19, 103661.

[7]. Cheemaa, N., Seadawy, A. R., Sugati, T. G., & Baleanu, D. (2020). Study of the dynamical nonlinear modified Korteweg–de Vries equation arising in plasma physics and its analytical wave solutions. Results in Physics, 19, 103480.

[8]. Kumar, S., Kumar, A., Abbas, S., Al Qurashi, M., & Baleanu, D. (2020). A modified analytical approach with existence and uniqueness for fractional Cauchy reaction–diffusion equations. Advances in Difference Equations, 2020(1), 28.

[9]. Vázquez, L., & Jafari, H. (2013). Fractional calculus: theory and numerical methods. Open Physics, 11(10), 1163-1163.

[10]. Wu, Y., Geng, X., Hu, X., & Zhu, S. (1999). A generalized Hirota–Satsuma coupled Korteweg–de Vries equation and Miura transformations. Physics Letters A, 255(4-6), 259-264.

[11]. Abazari, R., & Abazari, M. (2012). Numerical simulation of generalized Hirota–Satsuma coupled KdV equation by RDTM and comparison with DTM. Communications in Nonlinear Science and Numerical Simulation, 17(2), 619-629.

[12]. Gbodogbe, S. O. (2025). Harmonizing epidemic dynamics: A fractional calculus approach to optimal control strategies for cholera transmission. Scientific African, 27, e02545.

[13]. Akinyemi, L., & Huseen, S. N. (2020). A powerful approach to study the new modified coupled Korteweg–de Vries system. Mathematics and Computers in Simulation, 177, 556-567.

[14]. Lawal, O. W., & Loyinmi, A. C. (2011). The effect of magnetic field on MHD viscoelastic flow and heat transfer over a stretching sheet. Pioneer J. Adv. Appl. Math, 3(2), 83-90.

[15]. Idowu, K. O., & Loyinmi, A. C. (2023). THE ANALYTIC SOLUTION OF NON-LINEAR BURGERS–HUXLEY EQUATIONS USING THE TANH METHOD. Al-Bahir journal for Engineering and Pure Sciences, 3(1), 8.

[16]. Loyinmi, A. C., & Lawal, O. W. (2011). The asymptotic solution for the steady variable-viscosity free convection flow on a porous plate. Journal of the Nigerian Association of Mathematical Physics, 19.

[17]. Oluwafemi, W. L., Adedapo, C. L., & Sowunmi, O. S. (2017). Homotopy perturbation algorithm using laplace transform for linear and nonlinear ordinary delay differential equation. Journal of the Nigerian Association of Mathematical Physics, 41, 27-34.

[18]. Loyinmi, A. C., & Akinfe, T. K. (2020). Exact solutions to the family of Fisher's reaction-diffusion equation using Elzaki homotopy transformation perturbation method. Engineering Reports, 2(2), e12084.

[19]. Lawal, O. W., Loyinmi, A. C., & Ayeni, O. B. (2019). Laplace homotopy perturbation method for solving coupled system of linear and nonlinear partial differential equation. J. Math. Assoc. Niger, 46(1), 83-91.

[20]. Lot, S., Lawal, W. O., & Loyinmi, A. C. (2024). Magnetic Field's Effect on Two-phase Flow of Jeffrey and Non-Jeffrey Fluid With Partial Slip and Heat Transfer in an Inclined Medium. Al-Bahir Journal for Engineering and Pure Sciences, 4(1), 8.

[21]. Loyinmi, A. C., & Akinfe, T. K. (2020). An algorithm for solving the Burgers–Huxley equation using the Elzaki transform. SN Applied sciences, 2(1), 7.

[22]. Lawal, O. W., Loyinmi, A. C., & Hassan, A. R. (2019). Finite difference solution for Magneto hydrodynamics thin film flow of a third grade fluid down inclined plane with ohmic heating. J. Math. Assoc. Niger, 46(1), 92-97.

[23]. Mohammadi, F., Moradi, L., Baleanu, D., Jajarmi, A.: A hybrid functions numerical scheme for fractional optimal control problems: application to nonanalytic dynamic systems. J. Vib. Control 24, 5030–5043 (2018)

[24]. Lawal, O. W., Loyimi, A. C., & Erinle-Ibrahim, L. M. (2018). Algorithm for solving a generalized Hirota-Satsuma coupled KDV equation using homotopy perturbation transform method. Science World Journal, 13(3), 23-28.

[25]. Loyinmi, A. C., Sanyaolu, M. D., & Gbodogbe, S. (2025). Exploring the Efficacy of the Weighted Average Method for Solving Nonlinear Partial Differential Equations: A Study on the Burger-Fisher Equation. EDUCATUM Journal of Science, Mathematics and Technology, 12(1), 60-79.

[26]. Lawal, O. W., & Loyinmi, A. C. (2012). Magnetic and porosity effect on MHD flow of a dusty visco-elastic fluid through horizontal plates with heat transfer. J. Niger. Assoc. Math. Phys, 21, 95-104.

[27]. Loyinmi, A. C., Oredein, A. I., & Prince, S. U. (2018). Homotopy adomian decomposition method for solving linear and nonlinear partial differential equations. Tasued J. Pure Appl. Sci, 1, 254-260.

[28]. Idowu, K. O., Akinwande, T. G., Fayemi, I., Adam, U. M., & Loyinmi, A. C. (2023). Laplace Homotopy Perturbation Method (LHPM) for solving systems of N-dimensional non-linear partial differential equation. Al-Bahir Journal for Engineering and Pure Sciences, 3(1), 11-27.

[29]. Loyinmi, A. C., & Idowu, K. O. (2023). Semi-analytic approach to solving rosenau-hyman and korteweg-de vries equations using integral transform. Tanzania Journal of Science, 49(1), 26-40.

[30]. Lawal, O. W., & Loyimi, A. C. (2019). Application of new iterative method for solving linear and nonlinear initial boundary value problems with non local conditions. *Science World Journal*, *14*(3), 100-104.

[31]. Maturi, D. A. (2012). Homotopy perturbation method for the generalized Hirota-Satsuma coupled KdV equation. *Applied Mathematics*, *3*(12), 1983-1989.

[32]. Loyinmi, A. C., Erinle-Ibrahim, L. M., & Adeyemi, A. E. (2017). The new iterative method (NIM) for solving telegraphic equation. J. Niger. Assoc. Math. Phys, 43, 31-36.

[33]. Lawal, O. W., Loyinmi, A. C., & Arubi, D. A. (2017). Approximate solutions of higher dimensional linear and nonlinear initial boundary valued problems using new iterative method. J. Niger. Assoc. Math. Phys, 41, 35-40.

[34]. Loyinmi, A. C., Lawal, O. W., & Sottin, D. O. (2017). Reduced differential transform method for solving partial integro-differential equation. J. Niger. Assoc. Math. Phys, 43, 37-42.

[35]. Loyinmi, A. C., & Lawal, O. W. (2011). The asymptotic solution for the steady variable-viscosity free convection flow on a porous plate. Journal of the Nigerian Association of Mathematical Physics, 19.

[36]. Gokdogan, A., Yildirim, A., & Merdan, M. (2012). Solving coupled-KdV equations by differential transformation method. World Appl. Sci. J, 19(12), 1823-1828.

[37]. Jafari, H., & Firoozjaee, M. A. (2010). Homotopy analysis method for solving KdV equations. Surveys in Mathematics and its Applications, 5, 89-98.

[38]. Lu, D., Suleman, M., Ramzan, M., & Ul Rahman, J. (2021). Numerical solutions of coupled nonlinear fractional KdV equations using He’s fractional calculus. International Journal of Modern Physics B, 35(02), 2150023.

[39]. Jafari, H., Nazari, M., Baleanu, D., & Khalique, C. M. (2013). A new approach for solving a system of fractional partial differential equations. Computers & Mathematics with Applications, 66(5), 838-843.

[40]. Elzaki, T. M. (2011). On the connections between Laplace and Elzaki transforms. Advances in Theoretical and Applied mathematics, 6(1), 1-11.